Optically Transparent Polyelectrolyte−Silica Composite Materials: Preparation, Characterization, and Application in Optical Chemical Sensing

Yining Shi and Carl J. Seliskar*

Department of Chemistry, University of Cincinnati, Cincinnati, Ohio 45221-0172

Received September 24, 1996. Revised Manuscript Received December 31, 1996[⊗]

A series of polyelectrolyte-containing silica composite materials have been prepared by sol−gel processing. These optically transparent composites have been characterized by scanning electron microscopy and UV−visible spectrophotometry. These materials can be processed into monolithic disks and thin films. The thicknesses of spin-coated films of these materials on glass can be varied from 0.13 to 3.5 μm as determined by an optical interference method. These materials are ion exchangeable and less brittle than the parent silica glass due to the incorporation of the organic polyelectrolyte. These new composites retain the nanoscale porosity and optical transparency into the ultraviolet of the parent silica sol−gel glasses, making them attractive host matrixes for the immobilization of ionizable dye molecules and chemical reagents. An optical pH sensing platform (0.9 × 2.5 cm) based on the electrostatic immobilization of HPTS (8-hydroxy-1,3,6-pyrenetrisulfonic acid trisodium salt) in a PDMDAAC (poly(diallyldimethylammonium chloride))−silica composite film was fabricated and evaluated. The results clearly demonstrate that this platform is easy to construct with high batch reproducibility and can be regenerated by simple solution ion exchange. The platform is usable in both the modes of absorption and fluorescence, making it versatile. Having a fast response time (ca. ∼2 s to more than 2 units of pH change), the platform is also highly resistant to dye leaching and storage degradation over a period of months.

Introduction

Organically modified sol−gel materials have recently been of interest because of their potential use as solid-state dye laser media,[1−5] nonlinear optical substrates,[6−9] waveguides,[10−13] biomaterials,[14] and as components of chemical or biochemical sensors.[15−18] The organic modifiers incorporated in the sol−gel processed inorganic matrixes can be organic dyes,[1−9,15−18] synthetic polymers[10−13,19−23] including polyelectrolytes,[24,25] and biomacromolecules.[14−18] Several polyelectrolyte-containing silica sol−gel systems, e.g., ones incorporating polyacrylic acid (PAA) and poly(sodium styrenesulfonate) (NaPSS), have been described in the literature.[24,25] Unfortunately, these polyelectrolyte-modified silica materials are optically translucent or opaque due to phase separation, thus preventing their optical sensing applications. In a procedure that begins with a preformed polyelectrolyte film, Mauritz and co-workers[26] have made inorganic oxide impregnated Nafion nanocomposites. These authors have apparently not reported on the optical properties (UV−vis) of these polyelectrolyte-based composites. We have also been interested in developing synthetic polyelectrolyte-containing sol−gel processed materials that are suited for the fabrication of preconcentration-based and dye-based optical chemical sensors.[27]

* To whom correspondence should be addressed. E-mail: Carl.Seliskar@uc.edu.

[⊗] Abstract published in *Advance ACS Abstracts,* February 15, 1997.

(1) Rahn, M. D. *Appl. Opt.* **1995**, *34*, 8260.
(2) Zhao, C. F.; He, G. S.; Bhawalkar, J. D.; Park, C. K.; Prasad, P. N. *Chem. Mater.* **1995**, *7*, 1979.
(3) Lam, K.-S.; Lo, D.; Wong, K.-H. *Appl. Opt.* **1995**, *34*, 8260.
(4) Canva, M.; Georges, P.; Perelgritz, J.-F.; Brum, A.; Chuput, F.; Boilot, J.-P. *Appl. Opt.* **1995**, *34*, 428.
(5) Lin, H.-T.; Bescher, E.; Mackenzie, J. D. *J. Mater. Sci.* **1992**, *27*, 5523.
(6) Oviatt, H. W. Jr.; Shea, K. J.; Kalluri, S.; Shi, Y.; Steier, W. H.; Dalton, L. R. *Chem. Mater.* **1995**, *7*, 493.
(7) Bella, S. D.; Fragala, I.; Ratner, M. A.; Marks, T. J. *Chem. Mater.* **1995**, *7*, 400.
(8) Sanchez, C.; Lebeau, B.; Viana, B. *Proc. SPIE Sol−Gel Opt. III* **1994**, *2288*, 227.
(9) Kasemann, R.; Bruck, S.; Schmidt, H.; Kador, L. *Proc. SPIE Sol−Gel Opt. III* **1994**, *2288*, 321.
(10) Yoshita, M.; Prasad, P. N. *Chem. Mater.* **1996**, *8*, 235.
(11) Yoshita, M.; Prasad, P. N. *Appl. Opt.* **1996**, *35*, 1500.
(12) Motakef, S.; Suratwala, T.; Roncone, R. L.; Boulton, J. M.; Teowee, G.; Neilson, G. F.; Uhlmann, D. R. *J. Non-Cryst. Solids* **1994**, *178*, 31.
(13) Motakef, S.; Suratwala, T.; Roncone, R. L.; Boulton, J. M.; Teowee, G.; Neilson, G. F.; Uhlmann, D. R. *J. Non-Cryst. Solids* **1994**, *178*, 37.
(14) Chen, Z.; Samuelson, L. A.; Akkara, J.; Kaplan, D. L.; Gao, H.; Kumar, J.; Marx, K. A.; Tripathy, S. K. *Chem. Mater.* **1995**, *7*, 1779.
(15) Lev, O.; Tsionsky, M.; Rabinovich, L.; Glezer, V.; Sampath, S.; Pankratov, I.; Gun, J. *Anal. Chem.* **1995**, *67*, 22A.
(16) Dave, B. C.; Dunn, B.; Valentine, J. S.; Zink, J. I. *Anal. Chem.* **1994**, *66*, 1120A.
(17) Avnir, D.; Braun, S.; Lev, O; Ottolenghi, M. *Chem. Mater.* **1994**, *6*, 1605.
(18) Ellerby, L. S.; Nishida, C. R.; Nashida, F.; Yamanaka, S. A.; Dunn, B.; Valentine, J. S.; Zink, J. I. *Science* **1992**, *255*, 1113.
(19) Wen, J.; Wilkes, G. L. *Chem. Mater.* **1996**, *8*, 1667.
(20) Verghese, M. M.; Ramanathan, K.; Ashraf, S. M.; Kamalasanan, M. N.; Malhotra, B. D. *Chem. Mater.* **1996**, *8*, 822.
(21) Loy, D. L.; Shea, K. J. *Chem. Rev. (Washington, D.C.)* **1995**, *95*, 1431.
(22) Scherer, G. W.; David, I. A. *Chem. Mater.* **1995**, *7*, 1957.
(23) Wei, Y.; Wang, W.; Yang, D.; Tang, L. *Chem. Mater.* **1994**, *6*, 1737.
(24) Nakanishi, K.; Soga, N. *J. Non-Cryst. Solids* **1992**, *139*, 1.
(25) Nakanishi, K.; Soga, N. *J. Am. Ceram. Soc.* **1991**, *74*, 2518.
(26) Shao, P. L.; Mauritz, K. A.; Moore, R. B. *Chem. Mater.* **1995**, *7*, 192 and references therein.

S0897-4756(96)00495-4 CCC: $14.00

For optical chemical or biochemical sensing applications, the sol−gel derived inorganic materials generally serve as host matrixes for the immobilization of reagents (sensing dyes or biomolecules). Of the several available immobilization techniques, simple doping of the sol−gel precursor with reagents is gaining popularity because of its generality, simplicity, and effective maintenance of original reagent properties in the immobilized state.[15−18,28−37] However, no matter how attractive this simple process might be, it often results in slow leaching of reagents from the doped sol−gel matrixes in many dye- and indicator-based chemical sensors. On the other hand, negligible leaching of large molecular weight biomolecules has frequently been achieved in enzyme-based biosensors.[15−18] This is not surprising since dopants of low molecular weight are generally small enough in size, compared with the typical pore sizes of sol−gel network (≅10−100 Å for films deposited from sol−gel solutions),[15−18,38] to readily diffuse through the matrix. However, biomolecules of high molecular weight are large enough to be physically entrapped within the porous hosts.[15−18]

Although many sol−gel process parameters governing the pore size and its distribution in the final gel matrix (e.g., pH, H_2O:Si molar ratio, temperature, solvent, additives, etc.) have been identified,[15] achieving the needed balance between controlling the pore size for nonleaching of entrapped low molecular weight reagents and the preservation of rapid response time remains a vexing experimental problem. Thermally densified (smaller pore-size) dye-based sol−gel sensors do exhibit diminished dye leaching but that desirable characteristic has also been accompanied by long sensor response times.[34,35]

Despite several efforts aimed at the development of disposable sol−gel-derived sensors based on simple optical transmission,[17,30] problems which stem from the physically fragile nature of low-temperature sol−gel-processed materials also remain. For example, in addition to having inherently long response times for measurement (1−24 h),[29] sol−gel monolith-based sensors crack easily when exposed to aqueous solution.[15,33] In the case of sol−gel thin-film sensors used at normal incidence, it is difficult to fabricate crack-free films of thickness more than 1 μm[10−13,15,34] so that the optical path length is necessarily very short, thus resulting in greatly diminished sensitivity.[29]

Recently, Panusa et al.[39] have studied an ethanol-sensitive dye entrapped within a pure silica network. These authors circumvented the problem associated with dye decomposition in the pure silica matrix by using a PMMA (poly(methyl methacrylate))−Silica-(SiO_2) composite material. They then demonstrated the usefulness of this composite material for optical chemical sensing.

In this article we describe several new polyelectrolyte-SiO_2 sol−gel composite materials that are not only ion-exchangeable but also less fragile than the pure parent silica material. These new materials retain the nanoscale porosity and optical transparency of the parent sol−gel glass, and can be processed into monoliths and thin films of widely variable thickness. To demonstrate the usefulness of these materials as host matrixes for dye-based optical sensors, we have constructed and evaluated a prototype optical sensor based on the immobilization of the pH-sensitive indicator, HPTS (8-hydroxy-1,3,6-pyrenetrisulfonic acid trisodium salt), in a PDMDAAC (poly(diallyldimethylammonium chloride))−SiO_2 composite film spin-coated on a glass substrate. This prototype pH sensor can be used in either or both modes of absorption and fluorescence in conventional spectrophotometers. The sensor exhibits rapid response time, high stability, and excellent reproducibility.

Experimental Section

Materials. The following chemicals were used: tetraethyl orthosilicate (TEOS, Huls Petrarch Systems), poly(diallyldimethylammonium chloride) (PDMDAAC, Polysciences, 20 wt % aqueous solution), poly(acrylic acid) (PAA, Polysciences), poly(vinylbenzyltrimethylammonium chloride) (PVTAC, Scientific Polymer Products, 30 wt % aqueous solution), Nafion perfluorinated ion-exchange material, 5 wt % solution in mixture of lower aliphatic alcohols and 10% water (Aldrich), poly(styrenesulfonic acid) (PSSA, Polysciences, 30 wt % aqueous solution), 8-hydroxy-1,3,6-pyrenetrisulfonic acid trisodium salt (HPTS, Molecular Probes), tris(2,2′-bipyridyl)ruthenium(II) chloride hexahydrate (Aldrich), and potassium ferricyanide (Aldrich). All reagents were used as received without further purification. Precleaned glass microscope slides (75 × 25 mm, 1 mm nominal thickness) were purchased from Clay Adams and used for spin coating. pH buffer solutions were prepared by making 0.08 M NaH_2PO_4 (Aldrich) and 0.25 M K_2HPO_4 (Fisher Scientific) in 500 mL of deionized water (Barnstead water purification system) followed by adjustment, with HCl or NaOH, to the desired pH values. All aqueous solutions were prepared with deionized water.

Preparation of Silica Sol−Gel and Polyelectrolyte Stock Solutions. Silica sol−gel stock solutions were prepared according to a previously reported protocol[40] with slight modification. In brief, 4.0 mL of TEOS, 2.0 mL of deionized water, and 100 μL of 0.1 M HCl were combined in a sealed 30 mL vial and stirred at room temperature. After 3 h of stirring, a transparent and single-phase sol−gel solution resulted. This solution was used as the stock solution for further polyelectrolyte incorporation. Polyelectrolyte stock solutions consisted of either directly purchased solutions or solutions made by simple dilution with deionized water.

Preparation of Polyelectrolyte−SiO_2 Sol−Gel Composite Materials. Incorporation of polyelectrolytes into silica sol−gel processed materials was achieved by mechanically blending sol−gel stock solutions with polyelectrolyte aqueous solutions. The volume ratio of the appropriate polyelectrolyte solution to the silica sol−gel stock solution was chosen to control the composition of the composite materials. The polyelectrolyte contents in dried composites were estimated using the density values of the polyelectrolyte aqueous solu-

(27) Petit-Dominguez, M. D.; Shen, H.; Seliskar, C. J.; Heineman, W. R. *Anal. Chem*., in press.
(28) Yang, L.; Saavedra, S. S.; Armstrong, N. R. *Anal. Chem*. **1996**, *68*, 1834.
(29) Yang, L.; Saavedra, S. S. *Anal. Chem*. **1995**, *67*, 1307.
(30) Dunuwilla, D. D.; Torgerson, B. A.; Chang, C. K.; Bergland, K. A. *Anal. Chem*. **1994**, *66*, 2739.
(31) Lee, J. E.; Saavedra, S. S. *Anal. Chim. Acta* **1994**, *285*, 265.
(32) MacCraith, B. D.; O'Keeffe, G. O.; McDonagh, C.; McEvoy, A. K. *Electron Lett*. **1994**, *30*, 888.
(33) Samuel, J.; Strinkovski, A; Shalom, S.; Lieberman, K.; Ottolenghi, M.; Avnir, D.; Lewis, A. *Mater. Lett*. **1994**, *21*, 431.
(34) Kraus, S. C.; Czolk, R.; Reichert, J.; Ache, H. J. *Sensors Actuators B* **1993**, *15−16*, 199.
(35) Lacan, P.; Gall, P. L.; Rigola, J.; Lurin, C.; Wettling, D.; Guizard, G.; Cot, L. *Proc. SPIE Sol−Gel Opt. II* **1992**, *1758*, 464.
(36) MacGraith, B. D.; Ruddy, V.; Potter, C.; O'Kelly, B.; McGilp, J. F. *Electron. Lett*. **1991**, *27*, 1247.
(37) Ding, J. Y.; Shahriari, M. R.; Sigel, G. H. *Electron. Lett*. **1991**, *27*, 1560.
(38) Yoldas, B. E. *Proc. SPIE Sol−Gel Opt*. **1990**, *1328*, 296.
(39) Panusa, A.; Flamini, A.; Poli, N. *Chem. Mater*. **1996**, *8*, 202.
(40) Narang, U.; Prasad, P. N.; Bright, F. V.; Ramanathan, K.; Kumar, N. D.; Malhotra, B. D.; Kamalasanan, M. N.; Chandra, S. *Anal. Chem*. **1994**, *66*, 3139.

tions supplied by the manufacturer and the measured mass of the dried silica xerogel (23.5% of the initially selected mass of the sol−gel stock solution).

Preparation of Thin Films and Monolithic Disks. All sol−gel-derived thin films were prepared from freshly formulated polyelectrolyte-containing sol−gel stock solutions by spin-coating the surface of glass microscope slides. A typical procedure for the spin-coating of the films onto the glass slides was as follows: 200 μL of polyelectrolyte containing sol−gel solution was pipetted onto the surface of the glass slide which was then spun at 3000 rpm for 30 s. The film was then dried under ambient room conditions overnight or longer. In some cases, films were also baked in an oven at 120 °C for 1 h.

For Nafion-SiO_2 films, thicker films (~1 μm thickness) were also made by allowing coating solutions to concentrate by evaporation to about one-third of their original volume before spin-coating since the viscosity of the original solution was too low to obtain thick films.

Monolithic disks were formed by filling plastic Petri dishes with appropriate volumes of the polyelectrolyte containing sol−gel solutions and then aging the covered Petri dishes under ambient conditions.

Fabrication of HPTS-Immobilized pH Sensing Films. PDMDAAC−SiO_2 composite films coated on glass slides (2.5 × 7.5 cm) were chosen as the host matrixes for the immobilization of the pH-sensitive dye HPTS. All PDMDAAC−SiO_2 films used for dye immobilization were baked at 120 °C for 1 h prior to soaking them in ca. 200 mL of 2.0 μM HPTS aqueous solution overnight. HPTS-loaded films were equilibrated in 200 mL of pH 7.0 buffer for 30 min to remove any loosely adsorbed HPTS from the film or glass substrate. Buffer-washed films on slides were then rinsed with water and dried under ambient conditions overnight. The dried HPTS films on glass slides were cut with a diamond knife into smaller pieces (0.9 cm × 2.5 cm) to fit into conventional 1 × 1 cm spectrophotometer cuvettes.

Scanning Electron Microscopy (SEM). Scanning electron microscopy of the composite films spin-coated on glass substrates was accomplished using a Stereoscan 90 microscope (Cambridge Instruments) operated at 25 kV and a view tilt angle of 25°. To obtain information on the micron-scale homogeneity of the inner bulk film and the thickness of the films, a portion of each film specimen was removed with a razor blade leaving a step for cross-section examination. Film specimens were sputter-coated with ~300 Å of gold prior to examination.

UV−Visible Absorption Spectrophotometry. UV−visible absorption (transmission) spectra were determined using a Hewlett-Packard 8452A diode array spectrophotometer. Optical transparency of the polyelectrolyte−silica composite materials was characterized by taking spectra of monolithic disks (~1 mm thickness). The ion-exchange characteristics of films were studied by making timed absorption measurements of exchange materials within the films which were positioned at normal incidence in the instrument. All films studied in this manner were allowed to equilibrate with water for at least 1 h before being immersed in aqueous solutions containing the exchange ion.

Spatially distributed absorption measurements of dye-doped films were performed to evaluate the uniformity of films. These measurements were obtained by manually scanning film-coated slides in the plane perpendicular to the diode array source beam which had been iris-reduced to about 5 mm diameter. Measurements were taken point-by-point on the entire 75 mm × 25 mm area of films and the resulting data introduced to and analyzed within a commercial personal computer spreadsheet.

Absorption-based pH sensing with HPTS-loaded PDMDAAC−SiO_2 films on glass substrates (0.9 cm × 2.5 cm) was investigated using near-UV transmitting 1 × 1 cm plastic cuvettes. The HPTS-loaded substrates were placed vertically inside the cuvettes in contact with the wall such that the films faced the cavity of the cuvette. pH tests were carried out using small quantitative additions of acid or base solutions. The dynamic responses of the HPTS-loaded films were examined by recording the absorbance changes at 460 nm following step injections of solutions of varying pH. The pH values of the solutions resulting from such quantitative additions of base and acid were carefully calibrated by independently measuring equivalent solutions with a pH meter (Accomet pH meter 910, Fisher Scientific). Leaching of HPTS from doped films was assessed by measuring the change in absorbance of films at normal incidence during continuous treatment of the slides with a series of leaching solutions, i.e., buffers with pH 2.0, 7.0, and 10.0, as well as 1.0 M NaCl aqueous solution.

Measurements of Refractive Index and Film Thickness. For refractive index measurements thicker films were formed by double spin-coating at 3000 rpm or single spin-coating at 1000 rpm. Refractive indices of the composite films spin-coated on glass substrates were determined using a Bausch and Lomb Abbe refractometer and the double-image method of Schulz.[41] Values reported are averages of five measurements made at different points on films. Thicknesses of films on glass substrates were determined using an optical interference fringe method, described by Goodman,[42] based on a single UV−visible absorption spectrum of the film recorded at normal incidence.

The film thickness, t, was calculated using

$$t = \frac{M_{ab}\lambda_a\lambda_b}{2(\lambda_a - \lambda_b)(n_1^2 - \sin^2\theta_0)^{1/2}}$$

where λ_a and λ_b are the wavelengths of the two fringe extrema (minima or maxima), n_1 the refractive index of the bulk film, θ_0 the angle of incident measuring beam with respect to the normal to the film surface, and M_{ab} the number of fringes separating these extrema.

Fluorescence Measurements. The instrument for fluorescence measurements consisted of the following: an excitation source, ILC 300 W xenon lamp coupled to a 0.25 m Spex Minimate; an emission monochromator and detector, Spex 0.5 m 1870C monochromator and Hamamatsu R955 phototube with high-voltage power supply; and a Stanford dual-channel boxcar integrator system interfaced to an IBM PC/AT data logging station equipped with data acquisition and analysis software.

Fluorescence-based pH sensing of HPTS-loaded films was performed also in a 1 × 1 cm plastic cuvette and with the same configuration of film placement described for absorption measurements above. The only difference was that the cuvette was oriented so that the excitation beam (λ = 460 nm) was positioned to strike the film at an incidence angle of ~30° with respect to the outer wall of the cuvette. Fluorescence was then collected at an acute angle with respect to the excitation beam using a C Technology quartz fiber optic bundle placed a few millimeters away from the film surface. The dynamic responses of HPTS-loaded films to varying pH were studied at the fluorescence emission wavelength of 524 nm. All pH changes were accomplished using the procedures described above for absorption measurements.

Results and Discussion

General Characterization of Composite Materials. For optical applications, material transparency is of primary concern. This concern is especially applicable here since numerous polymer-SiO_2 composites examined to date are opaque or translucent due to phase separation of the organic polymeric and inorganic components.[24,25] Nonetheless, a number of important polyelectrolytes (Figure 1) have been incorporated by us into silica while retaining transparency. This has been accomplished by augmenting the low-temperature sol−gel method with a simple polymer-blending procedure.

(41) Schulz, L. G. *J. Chem. Phys.* **1949**, *17*, 1153.
(42) Goodman, A. M. *Appl. Opt.* **1978**, *17*, 2779.

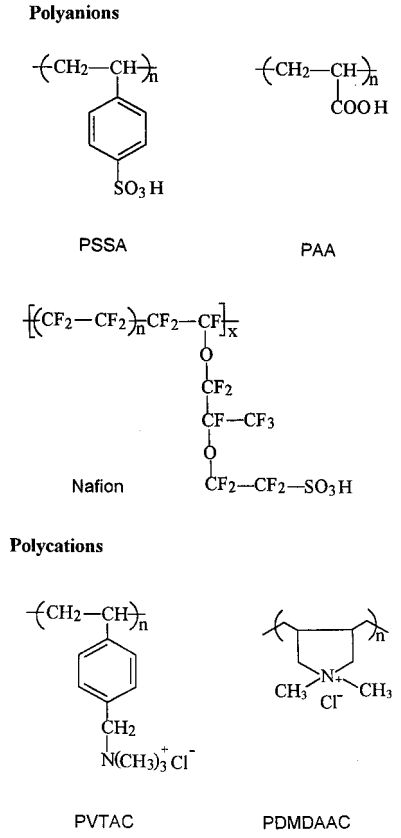

Figure 1. Chemical structures of the polyelectrolytes incorporated into SiO_2 by the low-temperature sol−gel process.

Certainly an important factor in producing not only transparent but also mechanically and chemically robust composites was the mass ratio between the polyelectrolyte and the silica-blending components. For the PDMDAAC−SiO_2 composite, although no precipitation was observed in blended solutions with very high polyelectrolyte contents (e.g., 80 wt %), 5 wt % is the upper limit of the PDMDAAC content in the blend solution for producing transparent and water-resistant materials. In addition, dried PDMDAAC−SiO_2 composites with a PDMDAAC content greater than 5 wt % in the blend solution always showed a thin layer of white powder on the surface of the materials, although the inner bulk section of the composite was clear and homogeneous. This white layer of powder is undoubtedly dried and silica-excluded PDMDAAC (vide infra). For the PVTAC-SiO_2 composite, highly transparent monoliths and films could be obtained without any limit on the polyelectrolyte content. However, 7.5 wt % in the blend solution is the upper limit of polyelectrolyte content for water-resistant composites. Despite having lower transmission in the UV region, dried PVTAC-SiO_2 monoliths with high PVTAC content (e.g., those made from 80 wt % in blend solution) do not show any white powder layer on their surfaces. Moreover, these polymer-rich monoliths are semiflexible. Like the PVTAC-SiO_2 composite, the Nafion−SiO_2 composite showed no upper limit of the polyelectrolyte content with respect to transparency. However, Nafion−SiO_2 spin-coated films demonstrated a limit of Nafion content beyond which island-shaped fragmented films were formed. Table 1 contains the compositions of the polyelectrolyte−SiO_2 composites which demonstrate the transparency and stability needed for typical applications in optical chemical sensing.

2

Table 1. Composition of Various Polyelectrolyte−SiO_2 Composites

polyelectrolyte	conc (wt %)	volume ratio[a]	content in blend solution (wt %)	content in dried composites (wt %)[b]
PAA	2.0	1:1	1.0	7.00
PSSA	10	1:1	5.0	31.8
Nafion	5.0	3:1	3.8	37.3
PDMDAAC	10	1:1	5.0	31.8
PVTAC	15	1:1	7.5	41.0

[a] With respect to freshly made SiO_2 sol−gel stock solution. [b] Estimations based on the dried SiO_2 gel being 23.5 wt % of the initial SiO_2 sol−gel solution.

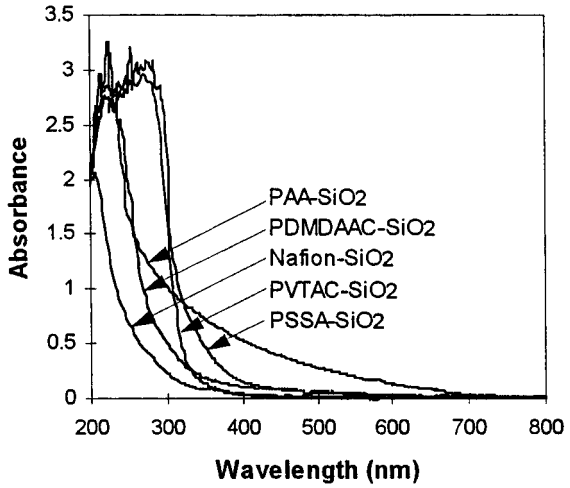

Figure 2. Absorbance spectra of monolithic forms of polyelectrolyte−SiO_2 composite materials. The monolith thickness in each case was ~1 mm. The spectrum of the translucent PAA−SiO_2 monolith is shown for comparison.

By careful selection of the sol−gel processing conditions and the compositions of the starting materials, we have produced a series of composites, containing either polycations or polyanions, which retain transparency even down to mid-UV wavelength region. Figure 2 shows the absorption spectra of selected composites in the form of monoliths. As shown in Figure 2, both the Nafion−SiO_2 and PDMDAAC−SiO_2 composites exhibit low absorption in the UV region (<300 nm), while both PVTAC−SiO_2 and PSSA−SiO_2 have strong absorptions in the near-UV region. All the composites shown (except PAA−SiO_2, which we have included as a comparison to previous work[24]) are highly transparent in the visible (>350 nm) to near-infrared wavelength region. We have not examined the absorption of these materials beyond 800 nm due to instrumental limitations. The strong UV-region absorptions of the PVTAC− and PSSA−SiO_2 composites stem from the π-conjugated aromatic structures of the respective polyelectrolytes themselves. It should be especially noted that we have prepared a transparent PSSA−SiO_2 composite. Previous workers[25] have reported preparing only a phase-separated translucent/opaque material using the sodium salt of the polyelectrolyte as the organic component. After repeating their work, we discovered that a transparent single-phase material can be made by making the composite with the acid form of the polyelectrolyte followed by ion-exchanging the resultant composite. Very thick monoliths (~3 mm) of PVTAC−SiO_2 and PSSA−SiO_2 showed slight brownish yellow colors which

we attribute to impurities in the commercial polymers used.

PAA possesses a comparably low UV absorption, and this is undoubtedly due to the lack of π-conjugated aromatic structure. Unfortunately, PAA−SiO_2 composites (Figure 2) are translucent or opaque. Previous workers found the composite to be opaque[24] at high concentrations of the polymer. Our translucent preparation of this material could be used for nonimaging or nonwaveguide sensor applications depending on short optical path lengths. The translucence of the PAA−SiO_2 composite is undoubtedly due to the incompatibility of the two components which results in phase separation of the system and thus light scattering. Although this incompatibility is not well understood, partial esterification of the PAA carboxylic groups during blending and aging, as suggested by Nakanishi and Soga,[24] may weaken the hydrogen-bonding and other favorable intermolecular interactions between the two components. In trying to test the hypothesis of Nakanishi and Soga, we added ethanol to the blended starting solution to increase esterification during the sol−gel process. We subsequently found an enhancement of the translucence of the cured composites. These results are consistent with previous work[24] which linked enhanced phase separation with the partial esterification of PAA. However, we also found that the transparency of PDMDAAC and PVTAC composites, both having quaternary ammonium functions, was sensitive to the presence of ethanol in the blended starting solutions.

Structural Characterization of the Composite Films. Emphasis was placed on the PDMDAAC−SiO_2 and Nafion−SiO_2 composites as representative materials containing polycationic and polyanionic components, respectively. To directly visualize the microstructure of the composites at a resolution of about 0.1 μm, we performed scanning electron microscopy studies on several samples. Figure 3 presents three SEMs acquired for the Nafion− and PDMDAAC−SiO_2 composites. In Figure 3A, direct evidence of a crack-free, flat surface on a homogeneous bulk film for the Nafion−SiO_2 composite is shown.

In contrast to the Nafion−SiO_2 composite, the PDMDAAC−SiO_2 composite exhibited a much different surface morphology. A freshly prepared film which has been dried at least overnight at ambient temperatures, but not treated with water, typically showed many heterogeneous particles scattered on the flat surface of the film. However, the bulk phase of the film was always homogeneous (Figure 3B). This interesting surface morphological feature does not persist after the film is treated with an aqueous solution nor does it reappear in time after initial washing. Indeed, a homogeneous film similar to that of the Nafion−SiO_2 film is obtained (Figure 3C) after water treatment of the original film. A closer examination of Figure 3B,C suggests that the small shallow craters visible on the top surface of the film in Figure 3C result from the removal of the heterogeneous particles that are loosely anchored on the surface of the film. On the basis of the above observations, we speculate that the micron-sized particles scattered on the top surface of the film are PDMDAAC which has been excluded from the film bulk phase as the composite gradually ages and shrinks. In addition, the particle-dotted surfaces of PDMDAAC−

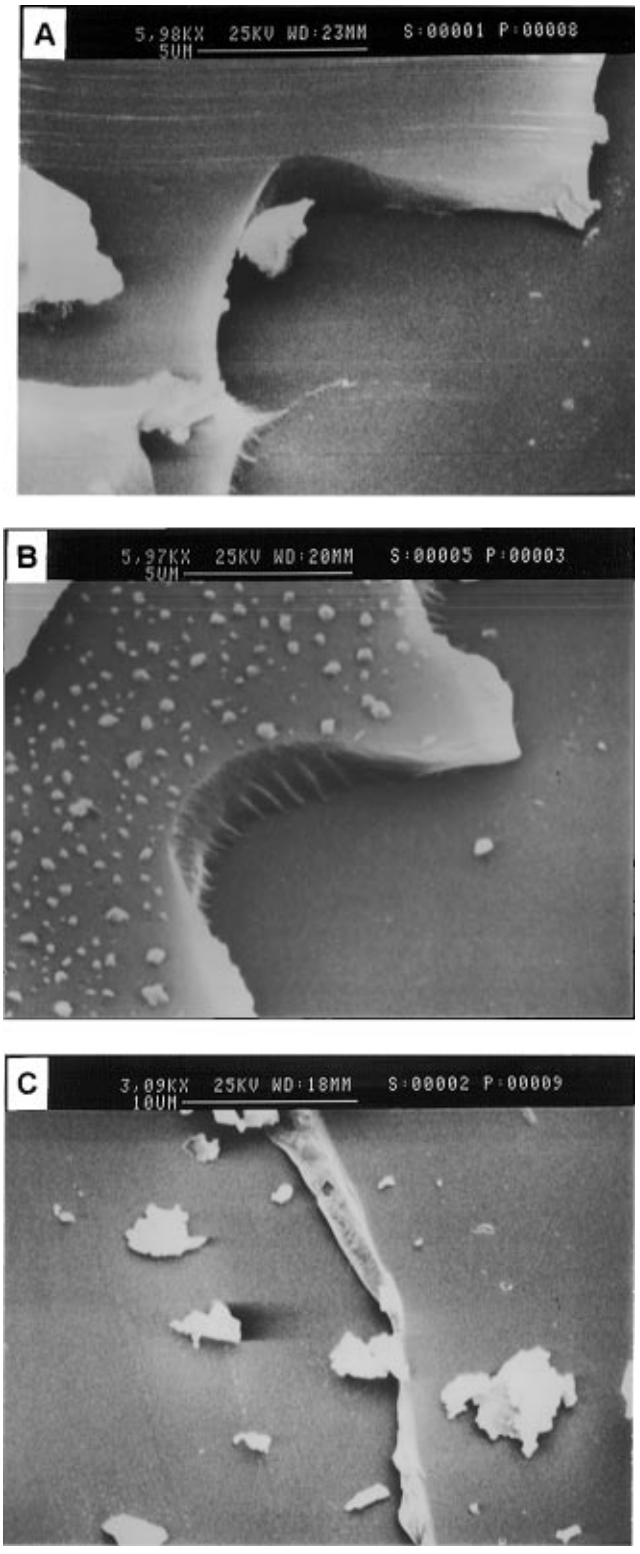

Figure 3. SEM micrographs of (A) a water-untreated Nafion−SiO_2 film, (B) a water-untreated (fully dry) PDMDAAC−SiO_2 film, and (C) a water-treated and HPTS-loaded PDMDAAC−SiO_2 film. The bottom portion of the material shown in each micrograph is the glass substrate. The large fragments in Figure 3A,C are scraps of the composite created during the formation of the gash in the film by razor blading.

SiO_2 films can be directly viewed under light microscopy. While viewing, the surface can be exposed to moist air under which condition the surface particles dissolve forming droplets of liquid. This behavior is consistent with the tenacity of the PDMDAAC polymer for water. Finally, this surface phenomenon has been

Table 2. Effects of Spin Rate and Dilution on the Film Thickness

spin rate (rpm)	dilution (v/v)[a]	fringe no.[b]	relative thickness (%)[c]	thickness (μm)[d]
500	1:0	22	100	3.45
1500	1:0	9	39	1.35
3000	1:0	5	26	0.90
3000	2:1	3	16	0.54
3000	1:1	1	3.8	0.13

[a] Ratio of coating solution/H_2O. [b]Counted in the wavelength range of 300−800 nm. [c] Calculated from eq 1 without knowing the n_1 value. [d] Calculated from eq 1 with $n_1 = 1.473$.

further substantiated by film optical interference measurements as described below.

Thickness Measurements on Films. Although the thicknesses of thin films can be determined using the more sophisticated methods of ellipsometry,[28] profilometry,[39] and surfometry,[40] the UV−vis absorption spectrophotometer can also be used to obtain sufficiently accurate film thickness measurements.[42,43] We have routinely used the absorption spectral method since it is rapid and nondestructive. Both the effects of the spin speed and dilution (viscosity) on film thickness are clearly demonstrated by measurements of film thickness. As an example, for PDMDAAC−SiO_2 (v/v = 1:1) films, thickness values were calculated based on the refractive index of the material (1.473 by Abbe refractometry). Table 2 shows representative effects of spin-speed and dilution on the thicknesses of these films. Compared with the effect of spin speed, dilution is a more sensitive means of controlling film thickness as it can dramatically decrease the viscosity of the coating solutions, particularly in the case of forming submicron films. As shown in Table 2, the thicknesses of the PDMDAAC−SiO_2 films can be controlled over the range 0.13−3.5 μm. This range of thicknesses is consistent with direct SEM thickness estimations on similar films.

The optical fringe method requires that the film be uniformly deposited on a flat substrate and that the film not appreciably scatter the light passing through it. Thus, this method can also serve as a sensitive diagnostic tool for the detection of surface heterogeneity and/or translucence in the bulk phase of the film. In the case of PDMDAAC−SiO_2 films, the freshly coated films dried under ambient conditions for only an hour are still wet. Such wet films always show sharp fringes. In addition, for polyelectrolyte-rich PDMDAAC−SiO_2 films, surface light-scattering accompanies the extended drying process which is accompanied by the loss of fringes in the spectra. After treatment with water (i.e., immersion in water for several minutes followed by air-drying), the films again show the characteristic fringed spectrum of clear homogeneous films and this persists indefinitely in time. As discussed in a prior section, the appearance of fringes with water exposure can be attributed to dissolution of excluded PDMDAAC particles present on the surface after initial drying of the films.

Film Incorporation of Dyes through Ion Exchange. All of the polyelectrolyte-SiO_2 composites were found to be ion-exchangeable. We have easily and rapidly incorporated many different ionizable chromophores and reagents into composite films by the ion-exchange process. In this paper we present some results of direct significance in chemical sensor applications. Figure 4 shows the incorporation of a divalent cation $Ru(bpy)_3^{2+}$ into a freshly prepared Nafion−SiO_2 film (~1 μm thick) by solution-phase cation exchange. The absorption spectral peaks of the film exposed to a solution of the cation (peaks at 286 and 450 nm) clearly indicate the incorporation of the colored cation into the film. A 1 μm water-equilibrated Nafion−SiO_2 film is saturated within about 4 min of solution exposure (see Figure 4, inset). The asymptotic upper limit of the concentration of $Ru(bpy)_3^{2+}$ incorporated in the film was calculated to be 0.35 M (mol of $Ru(bpy)_3^{2+}$ L of film), assuming that the solution-phase molar extinction coefficient at 450 nm (14 000 M^{-1} cm^{-1}) holds for the solid film medium. Finally, it should be noted that Nafion−SiO_2 films dried in air overnight and inserted **dry** into ion-exchange solutions showed a longer saturation time (typical time 1−2 h). This longer saturation time is presumably due to either or both a considerable change in the pore structure of the films or a long rehydration time needed for dry films.

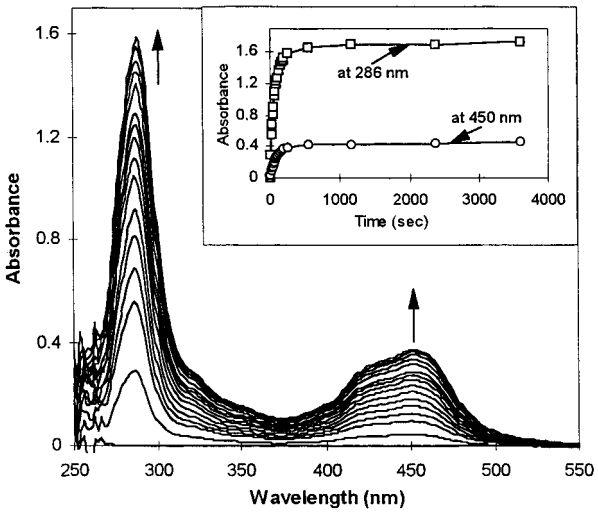

Figure 4. Absorbance spectral changes with increasing aqueous solution (0.05 mM, 40 mL) exposure time, indicating the incorporation of $Ru(bpy)_3^{2+}$ into a ~1.0 μm thick Nafion−SiO_2 film coated on 0.9 cm × 2.5 cm glass substrate. Spectra were recorded from 0 s (bottom curve) to 200 s (topmost curve) with a time interval of every 10 s for the first 11 spectra and every 20 s for the last 5 spectra. The inset in the figure is a plot of the absorbance at two peak wavelength positions versus time.

To evaluate the uniformity of $Ru(bpy)_3^{2+}$ distributed in the films, we have also conducted a series of spatially scanned absorption measurements on $Ru(bpy)_3^{2+}$-loaded films. Overall, such films are very uniformly loaded with the exchange cation: as an example, for one film and a total of 61 × 17 = 1037 surface measurements, A(286 nm) = 2.05 ± 0.087(3σ) and A(450 nm) = 0.261 ± 0.014(3σ) corresponding to a coefficient of variance, σ/x_{ave} of 1.5 and 1.8%, respectively. The most uniform zone in the film is located in the central area, which is evident from measurements at both 286 and 450 nm. Slight variations around the edges, especially the two short edges, corresponding to the greatest distance away from the spin rotor axis, could result from a thicker film in these regions formed during spin-coating.

Figure 5 shows the incorporation of a trivalent anion, $Fe(CN)_6^{3-}$, into a PDMDAAC−SiO_2 film by solution

(43) Simon, W.; Seiler, K. *Anal. Chim. Acta* **1992**, *266*, 73.

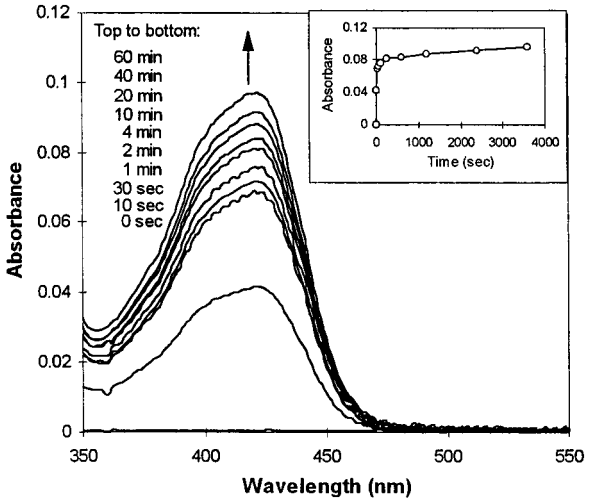

Figure 5. Absorbance spectra of a PDMDAAC−SiO_2 film (0.9 cm × 2.5 cm × ~1.0 μm) showing the incorporation of $Fe(CN)_6^{3-}$ from aqueous solution (0.025 M, 0.1 M NaOH, 40 mL). Spectra were recorded from 0 s (bottom curve) to 60 min (top curve) as shown. The inset is a plot of the absorbance at 420 nm versus time.

anion exchange. Anion-exchange saturation was found to occur within ca. 4 min (see inset, Figure 5) for initially wetted films even in the presence of a high concentration of hydroxide ions (0.1 M). Furthermore, the $Fe(CN)_6^{3-}$-loaded films were found to be rugged and resisted even 1 M alkali for long periods of time. The asymptotic limit of the concentration of $Fe(CN)_6^{3-}$ incorporated in the film was calculated to be 1.1 M, assuming that the solution molar extinction coefficient of 1020 M^{-1} cm^{-1} at 420 nm pertains to the film-loaded material.

Optical pH-Sensing Application. *pH Measurements.* To test the suitability of the new composites as host matrixes for pH dye immobilization, an optical sensor was constructed based on the ion exchange immobilization of HPTS in PDMDAAC−SiO_2. HPTS is a widely used pH indicator for fluorescence pH sensors because of its physiological pH range, high quantum yield, large Stokes' shift, and the presence of three negatively charged sulfonate groups available for electrostatic immobilization.[44] The pH sensor was fabricated on a glass platform which fitted into a conventional plastic cuvette, thus allowing use in commonly available spectrophotometers and fluorimeters.

Figure 6 shows the pH behavior of a HPTS-loaded film examined in absorption mode. The spectra for both the acid and base forms of the immobilized HPTS showed the expected maxima at 408 and 460 nm, respectively. The maximum at 408 nm shifts to longer wavelength (460 nm) as the pH increases (Figure 6A). The superimposed spectra acquired during pH change show a well-defined isosbestic point at 333 nm with a highly convergent (uncorrected) baseline. In turn, this behavior is indicative of insignificant dye leaching and a negligible change of film matrix background which is not easily achievable in comparable organic polymeric matrixes.[45] A plot of the absorbances at 408 and 460 nm against pH is shown in Figure 6B. The error bars

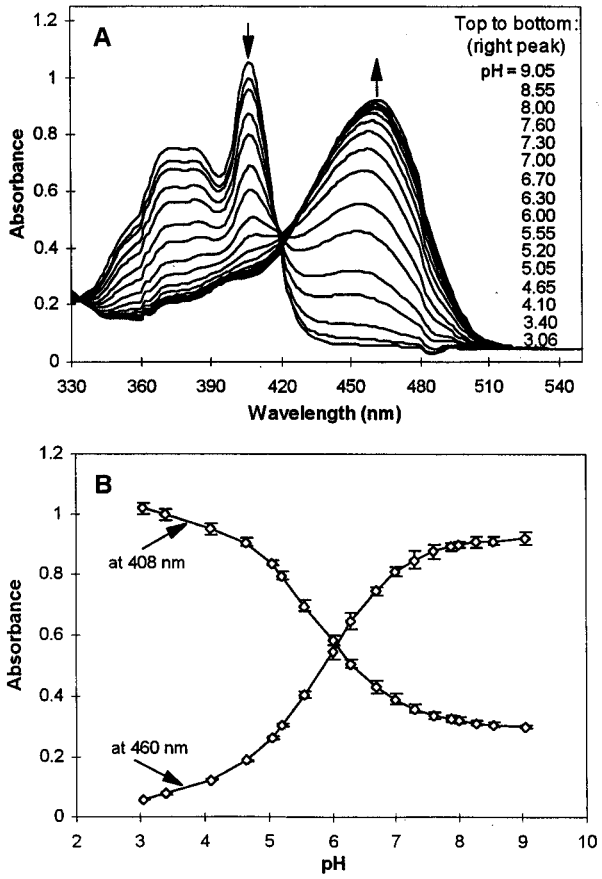

Figure 6. pH-dependent absorbance spectra (A) and the calibration curves at two wavelengths (B) for a HPTS-loaded PDMDAAC−SiO_2 film. The calibration data were compiled from measurements on five different films, and the error bars correspond to 1 standard deviation.

shown in the figure represent the standard deviation for five sets of data obtained on five different platforms. The relative standard deviation of the 18 pH measurements from pH 3.06 to 9.05 was 2.2%. The relatively high reproducibility of laboratory-made platforms might reasonably be attributed to the uniformity of the film formed by the spin-coating technique. This reproducibility may possibly be able to be further improved by carefully controlling the viscosity of the casting solutions and prescreening the platforms through scanning absorption measurement. It is noteworthy that one common drawback of the fiber optic chemical sensors is their poor batch reproducibility (between-device precision) resulting in a need for each device to be calibrated before use.[36,46−48] For the purposes of routine analytical use, it might be noted that compared with the measured variation of the acid form of immobilized HPTS at 408 nm, the variation in base form at 460 nm resulted in a larger linear variation region from pH 5.0 to 7.3 (correlation coefficient 0.99).

As an experimental alternative, the same HPTS-loaded PDMDAAC−SiO_2 platform can be easily used with an ordinary fluorimeter. Figure 7 shows the pH-dependent spectra of the platform operated in the mode

(44) Leiner, M. J. P.; Hartmann, P. *Sensors Actuators B* **1993**, *11*, 281.

(45) Chang, S, H.; Druen, S. L.; Garcia-Rubio, L. H. *Proc. SPIE* **1995**, *2388*, 540.

(46) Zhang, S.; Rolfe, P.; Wickramasinghe, Y. *Proc. SPIE Biochem. Med. Sensors* **1993**, *2085*, 22.

(47) Moreno, M. C.; Jimenez, M.; Conde, C. P.; Camara, C. *Anal. Chim. Acta* **1990**, *230*, 35.

(48) Fuh, M.-R.; Burgess, L. W.; Hirschfeld, T.; Christian, G. D. *Analyst* **1987**, *112*, 1159.

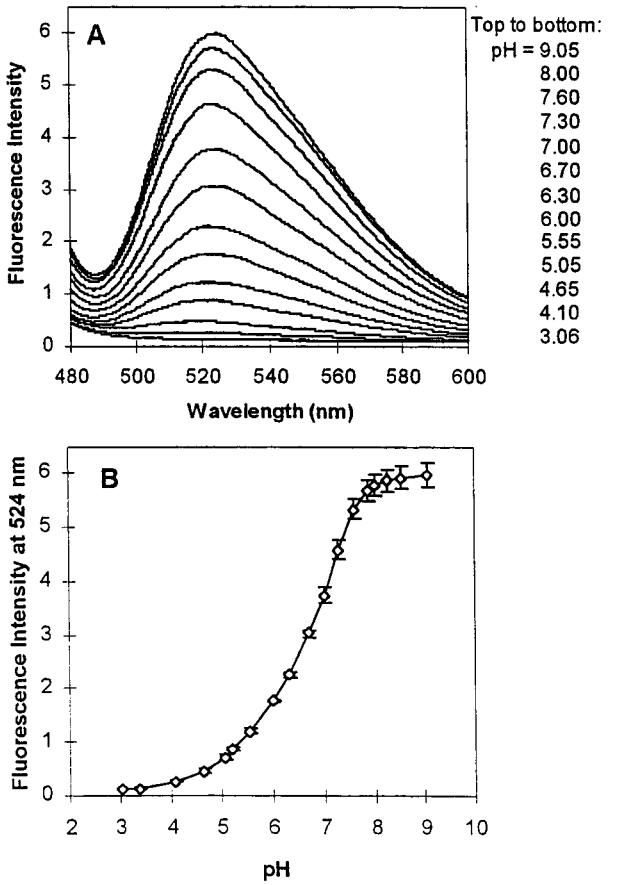

Figure 7. pH-dependent fluorescence spectra with excitation at 460 nm (A) and the resultant calibration curve (B) for a HPTS-loaded PDMDAAC−SiO_2 film. The calibration data were compiled from four sequential measurements with the same film. The error bars correspond to one standard deviation.

of fluorescence. Similar to the absorption spectra, the emission spectra (Figure 7A) change smoothly with pH and converge to a common baseline at wavelengths higher than 700 nm (not shown). The response of the fluorescence intensity to varying pH is given in Figure 7B. The error bars denote the standard deviation of the four sequences of fluorescence measurements performed on the same platform. The average coefficient of variation of the 18 measurements from pH 3.06 to 9.05 was 4.8%. For the purposes of routine analytical use, it might be noted that the linear dynamic range is over the region pH 6.0−8.0 with a correlation coefficient of 0.99. It is interesting that this pH range is more narrow and shifted to higher pH in comparison with that for absorption mode.

Response Times. Figure 8 shows typical response curves for HPTS-loaded PDMDAAC−SiO_2 platforms operated in the modes of absorption and fluorescence. The 90% response times for both modes of operation were ca. 2 s and independent of the magnitude of pH change as well as the direction of change, making the film platform one of the fastest optical chemical sensors reported to date. It seems that this rapid response time cannot just simply be ascribed to the porosity of the silica host matrix, since the typical response times for thin-film pH sensors based on the physical entrapment of dyes in pure silica matrixes are 15 s−60 min depending on thin film thickness (which varied from 0.085 to 0.35 μm) and processing conditions.[29,34,35] For comparison, we have also constructed a pH-sensing platform

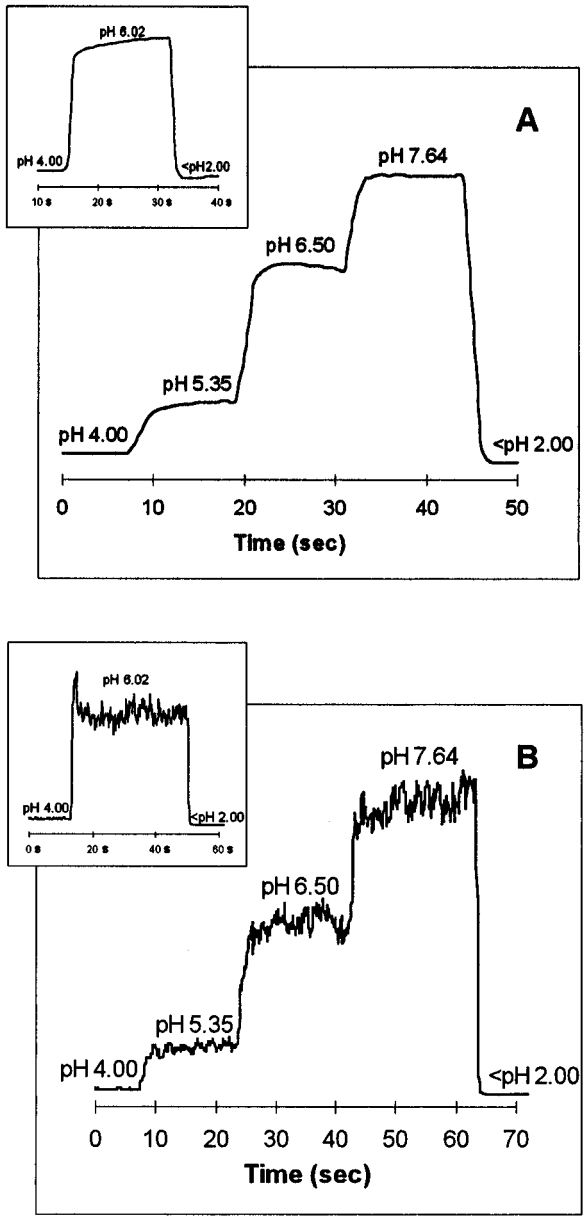

Figure 8. Dynamic response curves of the same HPTS-loaded PDMDAAC−SiO_2 film (0.90 μm thickness) recorded in the mode of absorption at 460 nm (A) and in the mode of fluorescence at 524 nm with excitation at 460 nm (B). The final solution values of pH are indicated for each pH step.

using physical entrapment of HPTS in the PDMDAAC−SiO_2 films. In this comparison we constructed a film of the same thickness (0.90 μm) but one which entrapped the dye HPTS. The dynamic response of this platform showed a much longer response time (up to 30 min), even though the dye concentration of the HPTS-entrapped film (0.15 M) was about 9 times less than that of the film for which the dye was immobilized by anion exchange (1.5 M).

A plausible general characterization of the sensor platform based on an ion-exchangeable composite film can now be made. The pore structure of the polyelectrolyte−SiO_2 film constitutes a network of interconnected channels for solution flow and low molecular weight solute diffusion. The outer surfaces of these channels contain exposed (polyelectrolyte) "docking" sites at which solution ions can exchange. Such electrostatically anchored ions remain totally and rapidly accessible to molecules contained within the solution

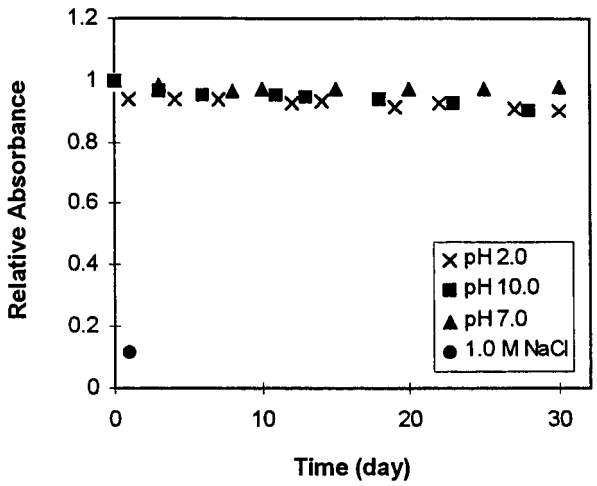

Figure 9. Results of studies of the leaching of HPTS from a PDMDAAC−SiO_2 film. The films which were spin-coated on 0.9 cm × 2.5 cm glass substrates were continuously immersed in 40 mL of buffer solutions or 1.0 M NaCl aqueous solutions over the indicated testing periods as indicated in the figure caption.

around them. The net result is that the dynamic response of a thin polyelectrolyte−SiO_2 film rivals that of a bulk solution−solid interface.

Stability. Since HPTS molecules are immobilized in the composite by ion exchange, leaching of the HPTS is a major concern. Figure 9 illustrates typical results of leaching studies done on HPTS-loaded PDMDAAC−SiO_2 platforms under a variety of buffer solution conditions. After 30 days of continuous treatment with buffer solutions, the signal loss due to the leaching of HPTS at pH 7.0 was only 2.1%, smaller than that at pH 2.0 (7.5%) and that at pH 10 (9.7%). It is to be noted that the majority of these losses occurred within the first 2−3 days of exposure. Overall, HPTS leaching under moderate pH conditions (e.g., pH 5−8) was not a major problem for this pH-sensing platform. The expected strong electrostatic interactions between the triply negatively charged HPTS ions and the positively charged quaternary ammonium groups of PDMDAAC in the composite must be major contributors to this excellent leaching stability. Consistent with the general experience with ion-exchange systems, treatment with 1.0 M NaCl aqueous solution produced a loss of 88% of the HPTS after only 1 day. The HPTS was totally lost within 2 days of exposure to this high salt concentration.

Longer exposure to high salt solution eventually resulted in delamination of the film from the glass substrate. While we have no direct measurements of film expansion and contraction under varying salt concentration exposures, it is possible that delamination of the film is a result of slight film contraction under high salt conditions. In addition, we currently have not carefully examined any low level leaching of polymer from the composites. Our continuing work on these new materials will address these issues.

Other concerns for the stability of optical chemical sensors are photostability and storage stability. A HPTS-loaded PDMDAAC−SiO_2 platform excited continuously at 460 nm in air for 5 h showed a 50% loss in HPTS fluorescence intensity at 524 nm. The same study done on an equivalent platform immersed in water showed no observable intensity loss over the same period of time. When not illuminated, the platform was found to be stable showing no absorption spectral changes for months of storage under ambient conditions. This result represents a significant improvement in the storage stability over other sensors based on HPTS immobilized in pure organic ion exchangers which suffer from more than 60% loss under dry storage conditions.[49]

Conclusions

We have prepared a series of new optically transparent polyelectrolyte−SiO_2 composite materials. Two of these composites, i.e., PDMDAAC−SiO_2 and Nafion−SiO_2, with the former representing the polycation−SiO_2 and the latter the polyanion−SiO_2 system, were chosen for more extensive structural characterization. The micron-scale homogeneity and mid-UV transparency of these two systems revealed by SEM and UV−visible spectrophotometry, respectively, suggested that it is possible to achieve high compatibility in polyelectrolyte−SiO_2 systems.

The new polyelectrolyte−SiO_2 composites have important advantages as host matrixes for thin-film optical chemical sensors based on dye immobilization. These materials demonstrated two features that the pure low-temperature-processed SiO_2 material does not posses: (1) ion exchangeability, by virtue of which ionizable dyes and reagents can be reversibly immobilized at high concentration and yet remain totally and rapidly accessible to solution analytes; (2) crack-free thick-film formation (>3 μm), by virtue of which longer optical path length and thus higher sensitivity can be achieved.

The usefulness of these new materials as host matrixes in particular for dye immobilization has been demonstrated by constructing and evaluating an optical pH sensor which could be operated in the modes of absorption and fluorescence. The clear advantages of such a platform design include (1) simple fabrication with high batch reproducibility, (2) low cost and hence disposability, (3) compatibility with conventional spectrophotometers, and (4) ease of usage.

Acknowledgment. We thank Professor William R. Heineman for helpful discussions and Dr. Jingyu Lian for assistance with the SEM measurements. This work was supported in part by the U.S. Department of Energy (Grant 86ER60487).

CM960495K

(49) Zhujun, Z.; Seitz, W. R. *Anal. Chim. Acta* **1984**, *160*, 47.